Hindawi Publishing Corporation
Journal of Nanomaterials
Volume 2012, Article ID 654379, 7 pages
doi:10.1155/2012/654379

Research Article

Influence of ITO-Silver Wire Electrode Structure on the Performance of Single-Crystal Silicon Solar Cells

Wern-Dare Jheng

Department of Mechanical Engineering, National Chin-Yi University of Technology, Number 57, Section 2, Chung-Shan Road, Taiping 411, Taichung, Taiwan

Correspondence should be addressed to Wern-Dare Jheng, jwd@ncut.edu.tw

Received 29 January 2012; Accepted 13 May 2012

Academic Editor: Arava Leela Mohana Reddy

This study aimed to explore the effect of various electrode forms on single-crystal silicon solar cells by changing their front and back electrode structures. The high light penetration depth of the Indium Tin Oxide (ITO) and the high conductivity of the silver wire that were coated on the single crystal silicon solar cells increased photoelectron export, thus increasing the efficiency of the solar cell. The experiment utilized a sol-gel solution containing phosphorus that was spin coated on single-crystal silicon wafers; this phosphorus also served as a phosphorus diffusion source. A p-n junction was formed after annealing at high temperature, and the substrate was coated with silver wires and ITO films of various structures to produce the electrodes. This study proposed that applying a heat treatment to the aluminum of back electrodes would result in a higher efficiency for single-crystal silicon solar cells, whereas single-crystal silicon solar cells containing front electrodes with ITO film coated with silver wires would result in efficiencies that are higher than those achieved using pure ITO thin-film electrodes.

1. Introduction

Since the industrial revolution, energy has been harnessed from petroleum and coal; however, these two sources are exhaustible. Moreover, large amounts of carbon dioxide emitted from fuel-generating energy have resulted in serious consequences, such as global warming [1]. As a result of countries around the world also beginning to place importance on this issue, the Kyoto Protocol was passed on December 11, 1997. The Protocol requested that 37 industrial countries and European Nations follow the 1990 standards to achieve a 5% reduction in greenhouse gas emissions from 2008 to 2012, and it was the first step in addressing global warming. The Copenhagen Summit in December, 2009 determined the global carbon reduction target for 2012–2017 in an attempt to prevent an irreversibly damaged climate. Presently, clean, renewable energy is the best solution to the global warming issues addressed by these initiatives. Because solar power is currently the cleanest and most feasible solution, several researchers are studying the solar cell for its potential in addressing these problems [2, 3].

Currently, commercial single-crystal silicon solar cells use silver grid electrodes as front electrodes [4, 5], which have a light obscuration rate of approximately 5–9%. Moreover, when electrons itinerate to the surface of n-type semiconductors, they are susceptible to capture by dangling bonds. Silica is most commonly used as the passivation layer and the antireflection layer for single-crystal silicon solar cells [6]. However, because it lacks a conducting path for electrons, it cannot be use for electrodes. Therefore, this study employs ITO with high transmittance and conductivity characteristics [7–10] as the antireflection layer and conducting electrodes for single-crystal silicon solar cells. This study also explores the effect of adding high-conductivity silver wire on single-crystal silicon solar cells.

2. Experiment

2.1. p-n Diode Production

2.1.1. Specimen Pretreatment [11]. The substrate was a silicon wafer (p-type) with the dimensions of $156 \times 156\,\text{mm}^2$ (lattice directions 100, resistivity $0.5\sim3\,\Omega$-cm, thickness $200\,\mu$m) cut into silicon chips of size $1.5 \times 1.5\,\text{cm}^2$. The following cleaning steps were performed.First, the silicon

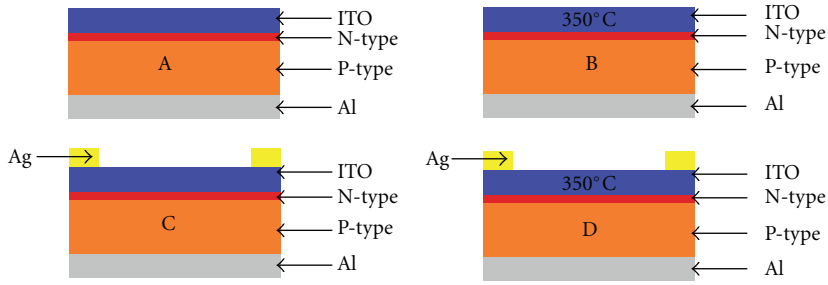

Figure 1: Single crystal silicon solar cells of different structure.

chips were immersed in a mixture of H_2SO_4 (98%) and H_2O_2 (30%) in a configured ratio of 3 : 1 for 10 minutes while the temperature was maintained at 80°C. The silicon chips were then removed and rinsed with deionized water. Next, the chips were immersed in a mixture of NH_4OH (29%), H_2O_2 (30%), and H_2O in a ratio of 1 : 1 : 5 for 10 minutes while the temperature was maintained at 80°C. The silicon chips were then rinsed again with deionized water for five minutes. Finally, the chips were immersed in buffer oxide etch (BOE) solution for one minute to remove the silicon oxide layer. The chips were blow-dried after cleansing.

2.1.2. Sol-Gel Configuration. This study used the sol-gel method for modulating phosphorus chemicals. The solution contained 4.69 g of polyethylene glycol, 18 g of ethanol, 0.563 g of H_2O, and 0.555 g of phosphorus pentoxide; the solution was stirred in a magnetic rotator for two hours to ensure that the solution was completely mixed.

2.1.3. Phosphorus Diffusion Process. The sol-gel configuration was spin coated onto single-crystal silicon. The spin coating was divided into two phases. The first phase consisted of a rotation speed of 2,000 rpm for a total of 10 seconds and was then followed by a second phase that consisted of a rotation speed of 6,000 rpm for a total of 10 seconds. The silicon was placed on a heating plate, where it underwent two-stage heating. During the first stage, a temperature of 120°C was maintained for 15 minutes to evaporate the solvent; during the second stage, a temperature of 200°C was maintained for 20 minutes. Subsequently, the silicon was placed inside a high-temperature furnace at a temperature of 900°C for 10 minutes so that it could undergo phosphorus diffusion. Upon completion of diffusion, a BOE solution was used to etch the phosphate glass for five minutes.

2.2. Electrode Production

2.2.1. Back Electrode Production. A magnetron sputter was used to coat the back of single-crystal silicon (of p-n structure) with aluminum. The sputtering power was 100 W, the work pressure was 5×10^{-3} Torr, and the sputtering time was 30 minutes; these parameters resulted in an aluminum thickness of 500 nm.

2.2.2. High-Temperature Sintering Process. The single-crystal silicon was thermally annealed to increase the bond strength between the metal and silicon, to export electrons and to produce back surface field structure. The annealing was performed at 650°C for 20 minutes.

2.2.3. Preparation of Transparent Conductive Film. An RF magnetron sputter was used to produce a coat of ITO. The sputtering power was 80 W, the work pressure was 3×10^{-3} Torr, and the sputtering time was 20 minutes. These parameters resulted in a 450 nm thick ITO film.

2.2.4. Transparent Conductive Film Annealing. Single-crystal silicon covered with an ITO electrode underwent a thermal annealing treatment to increase its light penetration depth and conductivity. The annealing temperature was maintained at 350°C for 30 minutes.

2.2.5. Silver Wire Coating. The front of single-crystal silicon was sputtered with silver wire using a magnetic sputter. The sputtering power was 50 W, the work pressure was 1×10^{-3} Torr, and the sputtering time was 10 minutes; these parameters produced a silver thickness of 300 nm.

2.3. Electrode Structure. This study explored the effect of electrode structure on single-crystal silicon via changing the front and back electrode production processes. The study examined four different electrode structures: A, B, C, and D. Each structure contained a heat-treated aluminum electrode and an aluminum electrode that had not been heat-treated. Structure A used ITO film as the front electrode, structure B used annealed ITO film as the front electrode, structure C used ITO film covered with silver wire as the front electrode, and structure D used annealed ITO film covered with silver wire as the front electrode. A, B, C, and D are solar cell structures, as shown in Figure 1.

3. Results and Discussion

3.1. Analysis of p-n Junction Properties. The resistance of single-crystal silicon after phosphorus diffusion was approximately 40 Ω/sq. with a mixed concentration of 10^{19} atom/cm^{-3}. The n-type silicon work function (W_S) was 4.07 eV, and the ITO work function of the experiment (W_m) was 3.8 eV, which met the conditions for metal-semiconductor ohmic contact ($W_m < W_S$).

The p-n junction solar cells are diodes that may be used to speculate the characteristics of single-crystal silicon

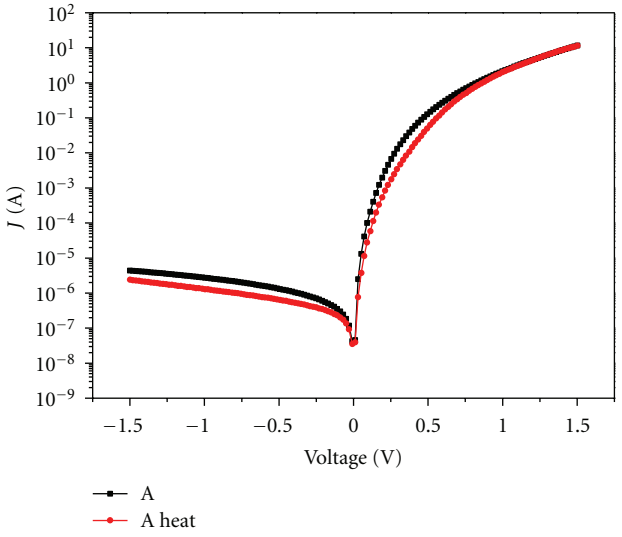

Figure 2: Dark current-voltage curve of structure A.

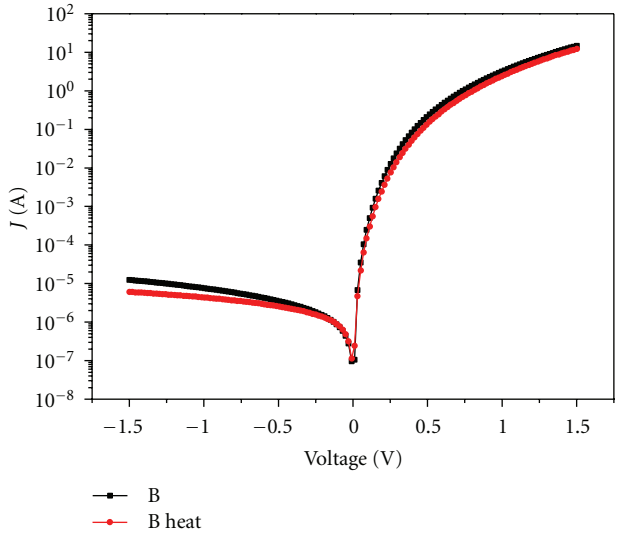

Figure 3: Dark current-voltage curve of structure B.

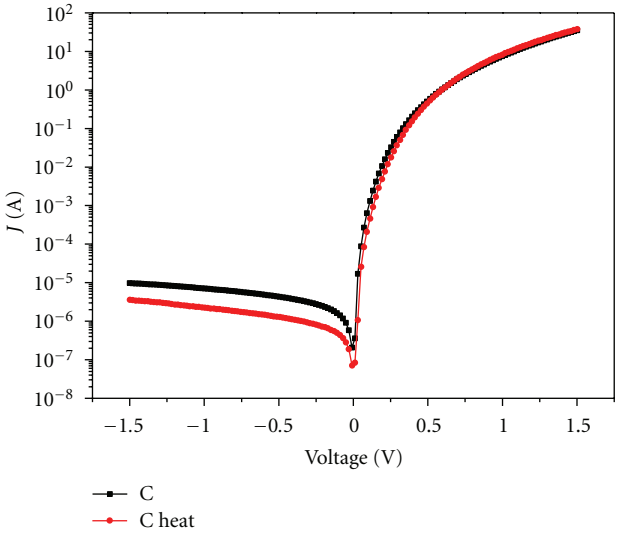

Figure 4: Dark current-voltage curve of structure C.

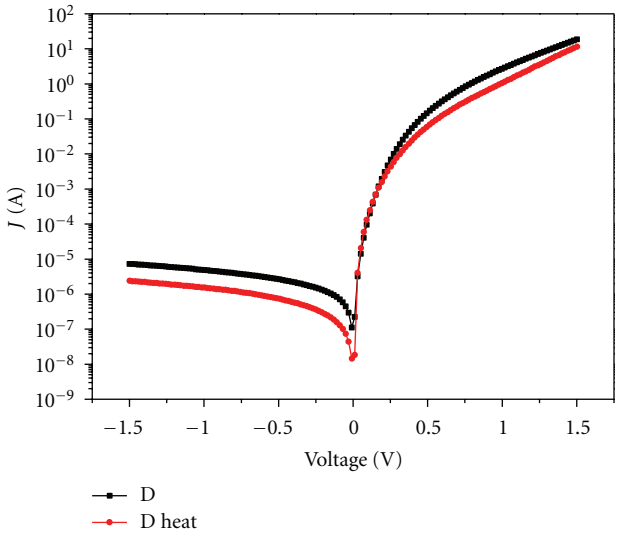

Figure 5: Dark current-voltage curve of structure D.

solar cells through dark current analysis of various electrode structures. The dark current-voltage curve in conjunction may be used to calculate the diode ideality factor (n value) [12, 13].

The dark current-voltage curve was measured on various electrode structures. Logarithmic coordinates were obtained from the current to obtain Figures 2, 3, 4, and 5 and then to obtain diode ideality factors (n). As shown in structure A in Figure 6, the n value calculated from the aluminum electrode before the heat treatment was 2.33, whereas the diode ideality factor following heat treatment of aluminum electrodes was 2.44. For single-crystal silicon solar cells with structure B, the n value calculated from the aluminum electrode before heat treatment was 1.72; the diode ideality factor after heat treatment of the aluminum electrodes was 2.32. For single-crystal silicon solar cells of structure C, the n value calculated from the aluminum electrode before heat treatment was 1.96; the diode ideality factor after heat treatment of the aluminum electrodes was 2.76. For single-crystal silicon solar cells of structure D, the n value calculated from the aluminum electrode before heat treatment was 2.11; the diode ideality factor after heat treatment of the aluminum electrodes was 2.81.

By performing the aforementioned analyses, we discovered that for the four different electrode structures, the diode ideality factor (n) increased when the aluminum electrodes were heat treated. Such a phenomenon implied that applying heat treatment to an aluminum back electrode would enhance the performance of p-n junction single-crystal silicon solar cells.

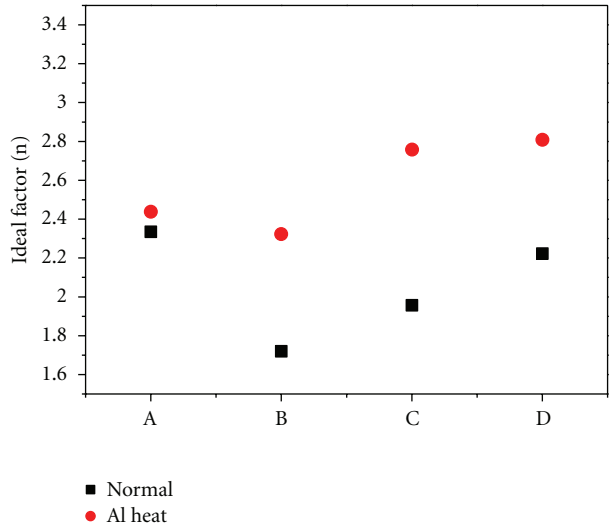

Figure 6: Ideality factors under different structure.

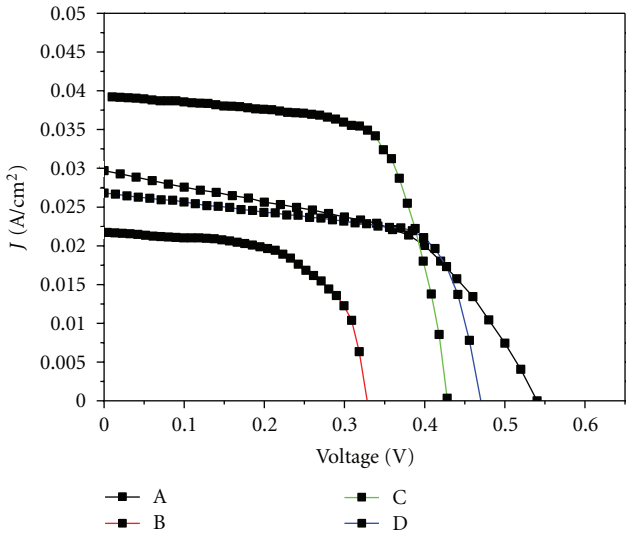

Figure 7: Current-voltage curve under different structure.

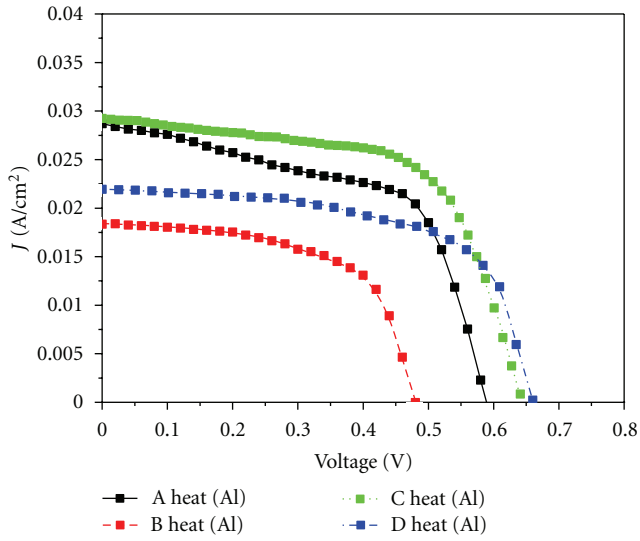

Figure 8: Current-voltage curve of aluminum undergone heat treatment under different structure.

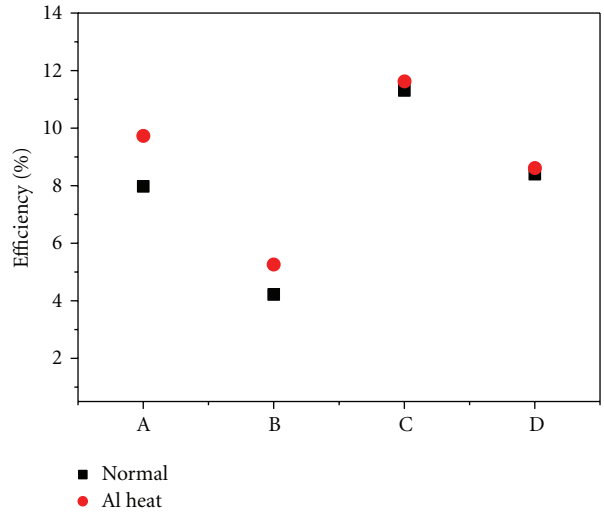

Figure 9: Efficiency map under different structure.

3.2. Analysis of Optoelectronic Properties. The light source employed by this study was an AM1.5, which has an incident light source intensity of 100 mW/cm^2. The current-voltage curve for this lighting is shown in Figures 7 and 8.

3.2.1. Effect of Front Electrode Structure on Optoelectronic Properties. This study first probed the optoelectronic properties of single-crystal silicon solar cells with two different structures: a front electrode using pure ITO film (structure A) and a front electrode using ITO film combined with silver wire (structure C). The data were compiled in Figures 9–11 according to Figures 7 and 8. Structure A resulted in an optoelectronic conversion efficiency of 7.98%, open-circuit voltage of 0.53 V, and short-circuit current of 29.748 mA/cm^2. In comparison, structure C yielded improved optoelectronic properties; the photoelectric conversion efficiency increased to 11.31%, the open-circuit voltage increased to 0.42 V and the short-circuit current increased to 39.214 mA/cm^2.

Subsequently, structures B and D with heat treatment applied to the ITO were compared. Structure D (covered with silver wire) resulted in an open-circuit voltage (0.47 V), short-circuit current (26.810 mA/cm^2) and optoelectronic conversion efficiency (8.40%) that were all higher than the open-circuit voltage (0.33 V), short-circuit current (21.527 mA/cm^2), and optoelectronic conversion efficiency (4.22%) that resulted from structure B.

These results show that ITO covered with silver wire promotes rapid export of photoelectrons and substantially improves its efficiency.

This study then examined the impact of ITO heat treatment on single-crystal silicon solar cells by comparing structure A with structure B and structure C with structure

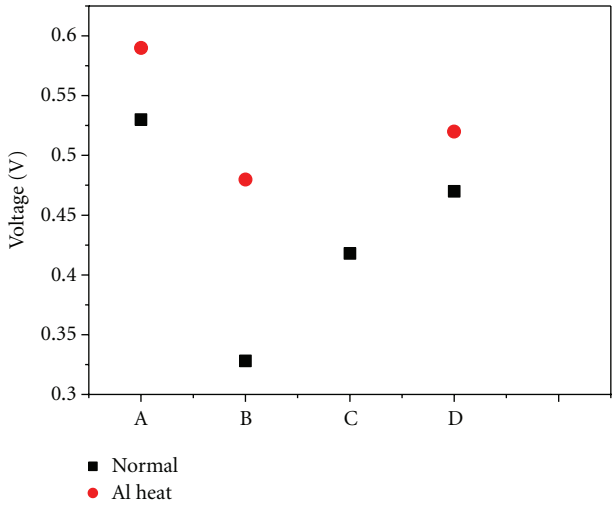

Figure 10: Open-circuit voltage under different structure.

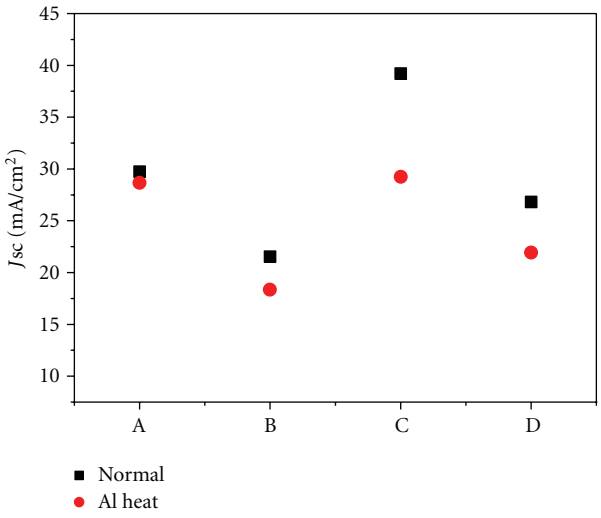

Figure 11: Short-circuit current under different structure.

D. The following results were obtained. The ITO film with structure A was used as the front electrode that exhibited higher efficiency; the optoelectronic conversion efficiency was 7.98%, the open-circuit voltage was 0.53 V and the short-circuit current was 29.748 mA/cm^2. In comparison, the ITO with structure B and a heat treatment of 350°C were used as front electrode that showed a lower efficiency; the optoelectronic conversion efficiency dropped to 4.22%, the open-circuit voltage dropped to 0.33 V and the short-circuit current dropped to 21.527 mA/cm^2. Next, the optoelectronic properties of structures C and D were compared The optoelectronic conversion efficiency of structure C was 11.31%, the open-circuit voltage was 0.42 V, and the short-circuit current was 39.214 mA/cm^2. Upon applying a heat treatment of 350°C to the ITO with structure D, the optoelectronic efficiency decreased to 8.40%, the open-circuit voltage increased to 0.47 V, and the short-circuit current decreased to 26.810 mA/cm^2. These results show that ITO causes single-crystal silicon solar cells to decline in overall efficiency upon undergoing a heat treatment of 350°C.

3.2.2. Effect of Heat Treating on the Aluminum Back Electrode. Figures 9–11 show that the aluminum electrode of structure A produced an open-circuit voltage of 0.53 V, short-circuit current of 29.748 mA/cm^2 and optoelectronic conversion efficiency of 7.98% before a heat treatment was applied. After applying a heat treatment of 650°C to the aluminum electrode, the open-circuit voltage increased to 0.59 V, the short-circuit current decreased to 28.664 mA/cm^2, and the optoelectronic conversion efficiency rose to 9.72%. The aluminum electrode of structure B yielded an open-circuit voltage of 0.33 V, a short-circuit current of 21.527 mA/cm^2, and an optoelectronic conversion efficiency of 4.22% before the heat treatment was applied. After applying the heat treatment of 650°C to the aluminum electrode, the open-circuit voltage increased to 0.48 V, the short-circuit current decreased to 18.355 mA/cm^2, and the optoelectronic conversion efficiency rose to 5.27%. The aluminum electrode of structure C produced an open-circuit voltage of 0.42 V, a short-circuit current of 39.214 mA/cm^2, and optoelectronic conversion efficiency of 11.31% before the heat treatment was applied. After applying a heat treatment of 650°C to the aluminum electrode, the open-circuit voltage increased to 0.64 V, the short-circuit current decreased to 29.250 mA/cm^2, and the optoelectronic conversion efficiency rose to 11.62%. The aluminum electrode of structure C produced an open-circuit voltage of 0.47 V, a short-circuit current of 26.810 mA/cm^2, and optoelectronic conversion efficiency of 8.40% before the heat treatment was applied. After applying the heat treatment of 650°C to the aluminum electrode, the open-circuit voltage increased to 0.66 V, the short-circuit current decreased to 21.935 mA/cm^2, and the optoelectronic conversion efficiency rose to 8.62%. These results show that ITO causes single-crystal silicon solar cells to decrease in short-circuit current after undergoing a heat treatment, whereas the open-circuit voltage and optoelectronic conversion efficiency will both increase.

3.2.3. Effect of Inside Impedance. The equivalent circuit for single-crystal silicon solar cells may be used to derive shunt resistance (R_{sh}), series resistance (R_s) and reverse saturation current (I_0) [14]. R_{sh} proportionally affects open-circuit voltage, whereas R_s inversely affects the shortcircuit current.

Figures 10 and 12 show that there is a significant correlation between R_{sh} and open-circuit voltage. Additionally, as shown in Figure 12, R_{sh} significantly increased after applying heat treatment to the aluminum electrode. For structure A, R_{sh} was 299.99 kΩ before applying heat treatment to the aluminum electrode, and R_{sh} rose to 383.71 kΩ after heat treatment. For structure B, R_{sh} was 120 kΩ before applying heat treatment to the aluminum electrode, and R_{sh} rose to 342.85 kΩ after heat treatment. For structure C, R_{sh} was 209.53 kΩ before applying heat treatment to the aluminum electrode, and R_{sh} rose to 379.29 kΩ after heat treatment. For structure D, R_{sh} was 356.73 kΩ before applying heat treatment to the aluminum electrode, and

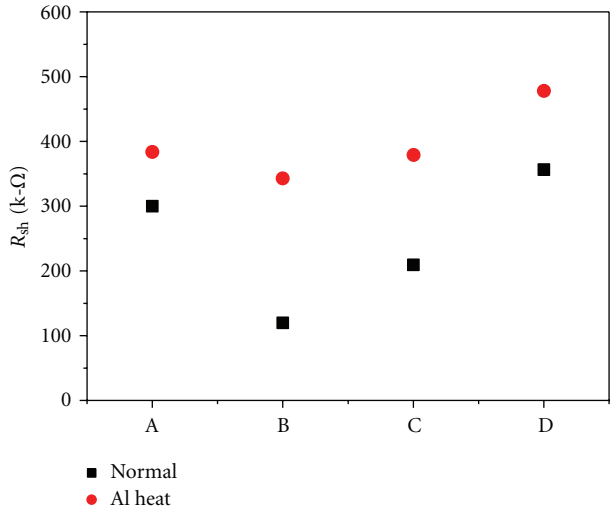

Figure 12: R_{sh} Comparison of parallel resistance under different structure.

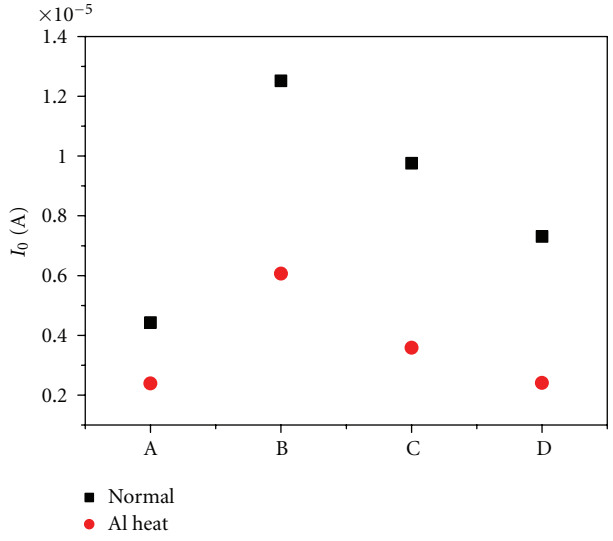

Figure 13: Comparison of reserve saturation current under different structure.

R_{sh} rose to 478.24 kΩ after heat treatment. These results show that R_{sh} increases after applying heat treatment to the aluminum electrode.

The increase in R_{sh} implied a better insulation between the front electrode and back electrode, which would also correspond to a lower reverse saturation current. Reverse saturation currents for different structures are compiled in Figure 13, which shows that the I_0 of structure A was initially 4.43 μA, but then decreased to 2.39 μA after heat treatment. The I_0 of structure B was initially 12.52 μA, but then decreased to 6.07 μA after heat treatment. The I_0 of structure C was initially 9.76 μA, but then decreased to 3.59 μA after heat treatment. The I_0 of structure D was initially 7.31 μA, but then decreased to 2.42 μA after heat treatment.

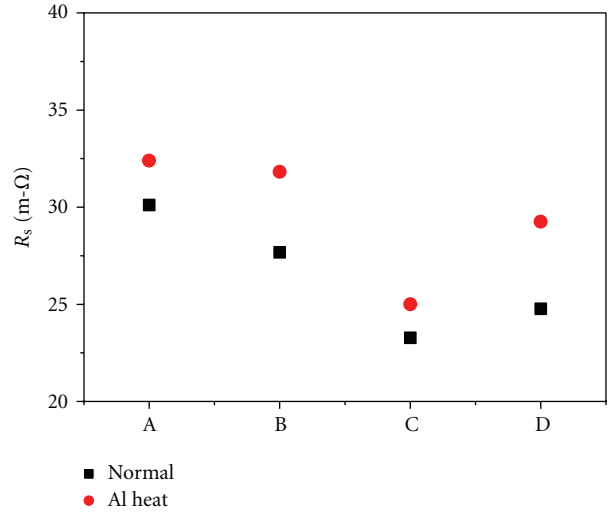

Figure 14: R_s Comparison of series resistance under different structure.

Figure 14 illustrates the series resistance (R_s) for different structures. Figures 11 and 14 show that R_s affects the short-circuit current (J_{sc}). After heat treatment, the R_s of structure A rose from 30.12 mΩ to 32.41 mΩ, and J_{sc} decreased from 29.748 mA/cm^2 to 28.664 mA/cm^2. After heat treatment, the R_s of structure B rose from 27.68 mΩ to 31.83 mΩ, and J_{sc} decreased from 21.527 mA/cm^2 to 18.355 mA/cm^2. After heat treatment, the R_s of structure C rose from 23.28 mΩ to 25 mΩ, and J_{sc} decreased from 39.214 mA/cm^2 to 29.250 mA/cm^2. After heat treatment, the R_s of structure D rose from 24.78 mΩ to 29.26 mΩ, and J_{sc} decreased from 26.810 mA/cm^2 to 21.935 mA/cm^2. These results show that R_s grew, whereas J_{sc} decreased after heat treatment of the aluminum electrode; this is due to the internal electronic transmission of the semiconductor encountering more obstacles, which thereby lowers the output current.

Moreover, in comparing structure A to structure C and structure B to structure C, we discovered that the electrode of ITO covered with silver wire results in a higher short-circuit current (J_{sc}) and a lower R_s than those produced by the electrode of pure ITO. This indicates that adding the electrode of silver wire reduces the R_s.

4. Conclusion

This study used the sol-gel method to prepare a phosphorus diffusion solution, which was spin coated onto the single-crystal silicon substrate using a 900°C heat diffusion process to form a p-n junction. This substrate was then covered with an ITO layer of variable structure and silver wire as the electrode. The impact of heat treatment on electrode structure was also examined in the study and yielded the following results.

(1) The average efficiency of single-crystal silicon solar cells increased after applying a 650°C heat treatment to the aluminum electrode.

(2) The efficiency decreased after applying a 350°C heat treatment to the ITO for 30 minutes, which resulted mainly from a decreasing shunt resistance and an increasing series resistance. This led to a decrease in both open-circuit voltage and short-circuit current, thereby lowering efficiency.

(3) When comparing the composite electrode of ITO and silver wire with pure ITO, the lower resistance of silver wire substantially enhanced the short-circuit current; however, it also reduced some of the open-circuit voltages. Overall, ITO covered with silver wire increased the optoelectronic efficiency of ITO.

(4) This study showed that the optimal front electrode structure was ITO covered with silver, which resulted in an 11.62% efficiency when a heat treatment of 650°C was applied to the aluminum metal of the back electrode.

References

[1] W. U. Huynh, J. J. Dittmer, and A. P. Alivisatos, "Hybrid nanorod-polymer solar cells," *Science*, vol. 295, no. 5564, pp. 2425–2427, 2002.

[2] W. He, T. T. Chow, J. Ji, J. Lu, G. Pei, and L. S. Chan, "Hybrid photovoltaic and thermal solar-collector designed for natural circulation of water," *Applied Energy*, vol. 83, no. 3, pp. 199–210, 2006.

[3] Y. Wang, Z. Fang, L. Zhu, Q. Huang, Y. Zhang, and Z. Zhang, "The performance of silicon solar cells operated in liquids," *Applied Energy*, vol. 86, no. 7-8, pp. 1037–1042, 2009.

[4] H. Katsumata, T. Ihara, and F. Tatekura, "New technology developments of solar cell fabrication by NEDO," in *Proceedings of the 24th IEEE Photovoltaic Specialists Conference. Part 2*, pp. 2240–2246, December 1994.

[5] N. B. Mason, T. M. Bruton, and M. Balbuena, "Laser grooved buried grid silicon solar cells from pilot line to 50 MWp manufacture in ten years," in *PV in Europe, Plenary Paper*, pp. 227–229, Rome, Italy, October 2002.

[6] K. R. McIntosh, N. C. Shaw, and J. E. Cotter, "Light trapping in sunpower's A-300 solar cells," in *Proceedings of the 19th European Photovoltaic Solar Energy Conference*, Paris, France, 2004.

[7] J. A. Amick, G. L. Schnable, and J. L. Vossen, "Deposition techniques for dielectric films on semiconductor devices," *Journal of Vacuum Science and Technology*, vol. 14, no. 5, pp. 1053–1063, 1977.

[8] I. Hamberg and C. G. Granqvist, "Evaporated Sn-doped In2O3 films: basic optical properties and applications to energy-efficient windows," *Journal of Applied Physics*, vol. 60, no. 11, pp. R123–R160, 1986.

[9] J. D. Rancourt, *Optical Thin Films: User's Handbook*, 1987.

[10] C. G. Granqvist, *Handbook of Inorganic Electrochromic Materials*, 1995.

[11] W.-D. Jheng and C. W. Chen, "Improve the efficiency of silicon solar cells by ITO-silver electrode structure," *ECS Transactions*, vol. 33, pp. 57–60, 2011.

[12] A. Jain and A. Kapoor, "Exact analytical solutions of the parameters of real solar cells using Lambert W-function," *Solar Energy Materials and Solar Cells*, vol. 81, no. 2, pp. 269–277, 2004.

[13] A. Jain and A. Kapoor, "A new method to determine the diode ideality factor of real solar cell using Lambert W-function," *Solar Energy Materials and Solar Cells*, vol. 85, no. 3, pp. 391–396, 2005.

[14] M. Bashahu and P. Nkundabakura, "Review and tests of methods for the determination of the solar cell junction ideality factors," *Solar Energy*, vol. 81, no. 7, pp. 856–863, 2007.